General Disclaimer

One or more of the Following Statements may affect this Document

- This document has been reproduced from the best copy furnished by the organizational source. It is being released in the interest of making available as much information as possible.

- This document may contain data, which exceeds the sheet parameters. It was furnished in this condition by the organizational source and is the best copy available.

- This document may contain tone-on-tone or color graphs, charts and/or pictures, which have been reproduced in black and white.

- This document is paginated as submitted by the original source.

- Portions of this document are not fully legible due to the historical nature of some of the material. However, it is the best reproduction available from the original submission.

NASA Technical Memorandum 84420

Determining the Operating Characteristics of an Ultraviolet Interferometric Spectrometer

C. L. Parsons

July 1983

National Aeronautics and Space Administration

Goddard Space Flight Center
Wallops Flight Facility
Wallops Island, Virginia 23337

NASA Technical Memorandum 84420

Determining the Operating Characteristics of an Ultraviolet Interferometric Spectrometer

C. L. Parsons

NASA Goddard Space Flight Center
Wallops Flight Facility
Wallops Island, Virginia 23337

National Aeronautics and
Space Administration

Goddard Space Flight Center
Wallops Flight Facility
Wallops Island, Virginia 23337

DETERMINING THE OPERATING CHARACTERISTICS OF AN ULTRAVIOLET INTERFEROMETRIC SPECTROMETER

C. L. Parsons
NASA Goddard Space Flight Center
Wallops Flight Facility
Wallops Island, VA 23337

INTRODUCTION

A prototype interferometric spectrometer system is being built by NASA to explore the potential of the technique for applications involving the visible and near-ultraviolet portions of the electromagnetic spectrum. As described in the paper by Parsons, Gerlach, and Whitehurst (1982), which will hereafter be referred to as PGW, the system is limited only by the frequency bandpass of the optical components used in the system, the quality of the optical components, and ultimately by the memory capacity of the computer. In PGW, however, the tradeoff between the wavenumber resolution of the produced spectrum, the bandpass limits of the optics, and the number of samples obtained from the interferogram were not delineated explicitly. The prototype Ultraviolet Interferometric Spectrometer (UVIS) instrument is expected to be configured several different ways to ascertain its suitability for various applications. To exploit its inherent flexibility, a reference document containing the parameter tradeoffs involved would be very useful. This paper is designed to be that reference.

BACKGROUND

The Interferogram

In PGW, the transform pair linking the wavenumber, σ, and path difference, x, domains was derived and found to be

$$\gamma(x) = \int_{-\infty}^{\infty} P(\sigma) e^{2\pi i \sigma x} \, d\sigma \qquad (1a)$$

$$P(\sigma) = \int_{-\infty}^{\infty} \gamma(x) e^{-2\pi i \sigma x} \, dx \qquad (1b)$$

where $\gamma(x)$ is the interferogram, or interference pattern, produced by the spectrometer when exposed to an incoming light beam having the spectral shape $P(\sigma)$. In actuality, of course, it is not possible to perform the integral calculations because the spectrum is too complex to permit closed-form solutions. Therefore, the integral transforms must in fact be replaced by a discrete Fourier transform pair. In this section, this relationship will be derived so that the pertinent parameters for interferometric spectroscopy and their interconnections can be described mathematically.

Figures 1 and 2 show graphically the steps in the path difference and wavenumber domains, respectively, that carry the interferogram and incoming spectrum at the top to the recovered discrete spectrum at the bottom. Each step will be discussed in detail and sequentially. The starting point is the production of the interferogram $\gamma(x)$ by the optical interference produced in the Michelson interferometer. Therefore, the linkage between Figures 1a and 2a is the optics in the instrument.

Once the path difference signal is produced, it must be captured in some way and this is done using an analog-to-digital converter. In the next section, the technique used to produce samples evenly spaced in path difference will be described in more detail. The sampling process can be described by the equation

$$\gamma(x)\Delta(x) = \gamma(x) \sum_{k=-\infty}^{\infty} \delta(x-k\Delta x) \tag{2}$$

where Δx is the path difference interval between samples. Using the transform pair relationship,

$$\sum_{k=-\infty}^{\infty} \delta(x-k\Delta x) \leftrightarrow \frac{1}{\Delta x} \sum_{k=-\infty}^{\infty} \delta\left(\sigma - \frac{k}{\Delta x}\right) \tag{3}$$

it is seen that sampling in the path difference domain is equivalent in the wavenumber domain to convolution of the spectrum by a series of delta functions spaced apart in wavenumber by multiples of $\frac{1}{\Delta x}$.

Figures 1c and 2c illustrate (2) and

$$P(\sigma) * \frac{1}{\Delta x} \sum_{k=-\infty}^{\infty} \delta\left(\sigma - \frac{k}{\Delta x}\right) \tag{4}$$

respectively.

Sampling Theorem

The sampling theorem has a deep significance in communication theory and other scientific disciplines involving measurements of signals at discrete intervals. It states that a bandlimited signal which has no wavenumber components above σ_{max} cm^{-1} is uniquely determined by its values at uniform intervals less than $\frac{1}{2\sigma_{max}}$ cm apart. To capture the spectrum in Figure 2a that created the interferogram in Figure 1a, the sampling illustrated in Figure 1b must be done at path difference intervals less than or equal to $\frac{1}{2\sigma_{max}}$ cm. That is,

$$\Delta x \leq \frac{1}{2\sigma_{max}} \tag{5}$$

For the case of equality, the sampling rate is at the Nyquist interval. In (4) then, the spectrum is replicated at intervals of $2\sigma_{max}$.

Truncation

Of course, the sampling process cannot be continued for an indefinite period of time. If for no other reason, there will be an upper limit on the number of samples that the system computer can process. Therefore, the series of sampling triggers is truncated by either the rectangular pulse shown in Figure 1d or by some other functional form that eliminates sampling for path differences in excess of $\pm \frac{X_t}{2}$ from ZPD. X_t is the total path difference allowed by this truncation process. If the pulse in Figure 1d is labelled A(x), then its transform is given by

$$A(\sigma) = X_t \frac{\sin \pi\sigma X_t}{\pi\sigma X_t} = X_t \, \mathrm{sinc}(\sigma X_t) \tag{6}$$

The sinc function has its first zero at $\sigma = \frac{1}{X_t}$ and oftentimes this wavenumber is termed the resolution $\Delta\sigma$ of the procedure. Figure 2d depicts the sin x/x type behavior and in Figure 2e the convolution of the preceding signal with $A(\sigma)$ is shown. Normally, instead of the rectangular pulse, a tapered function known as the apodization function is used. A variety exist with each having attributes such as low sidelobes or fast rolloff that are attractive for particular applications. The particular form used for UVIS was described in PGW. For this study, the merits are not important; it is sufficient to use the rectangular truncation in the rest of the analysis. In summary, at this point in the development, the signal in the path difference domain can be described by

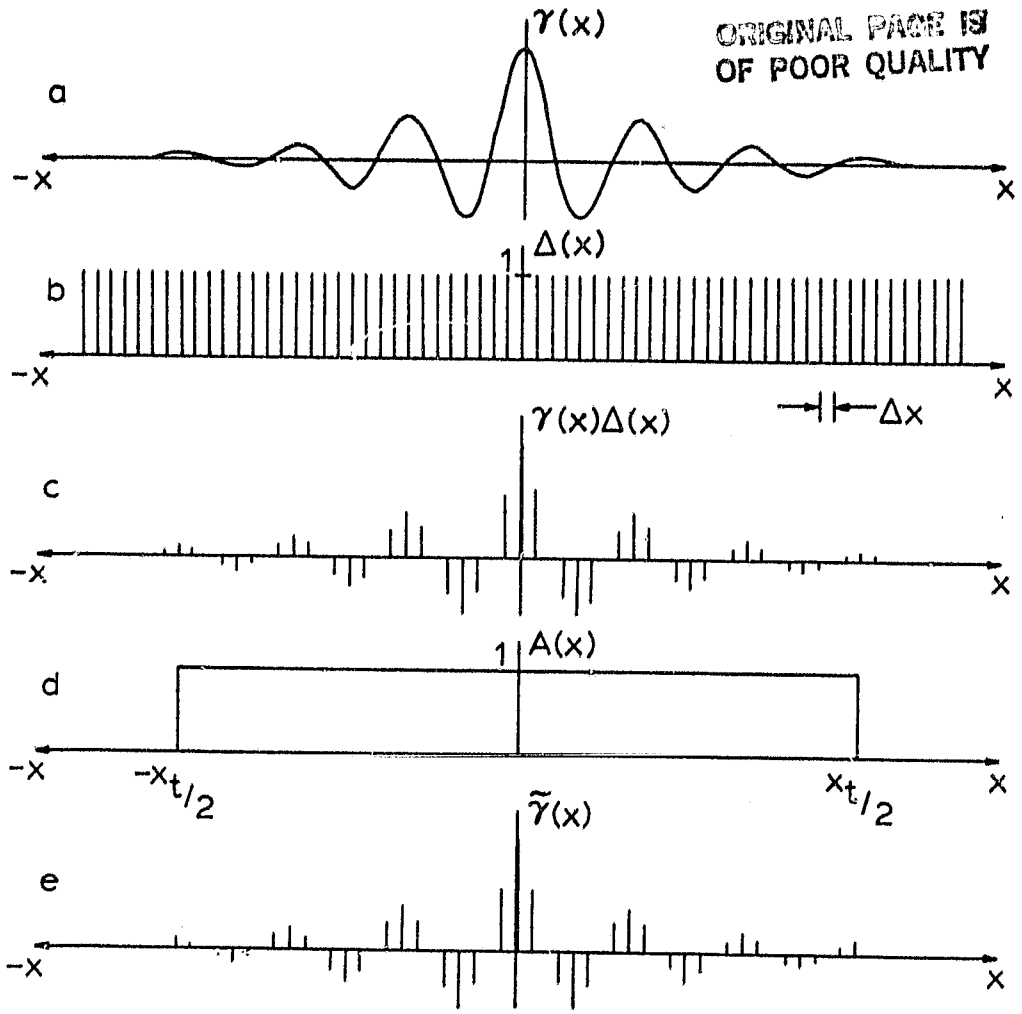

Figure 1. Fourier transform spectrometry signals in the path difference, x, domain. (a) The interferogram. (b) An infinite sequence of sampling triggers spaced Δx path difference units apart. (c) The interferogram after sampling. (d) The apodization function (here represented by simple truncation). (e) The sampled interferogram after truncation.

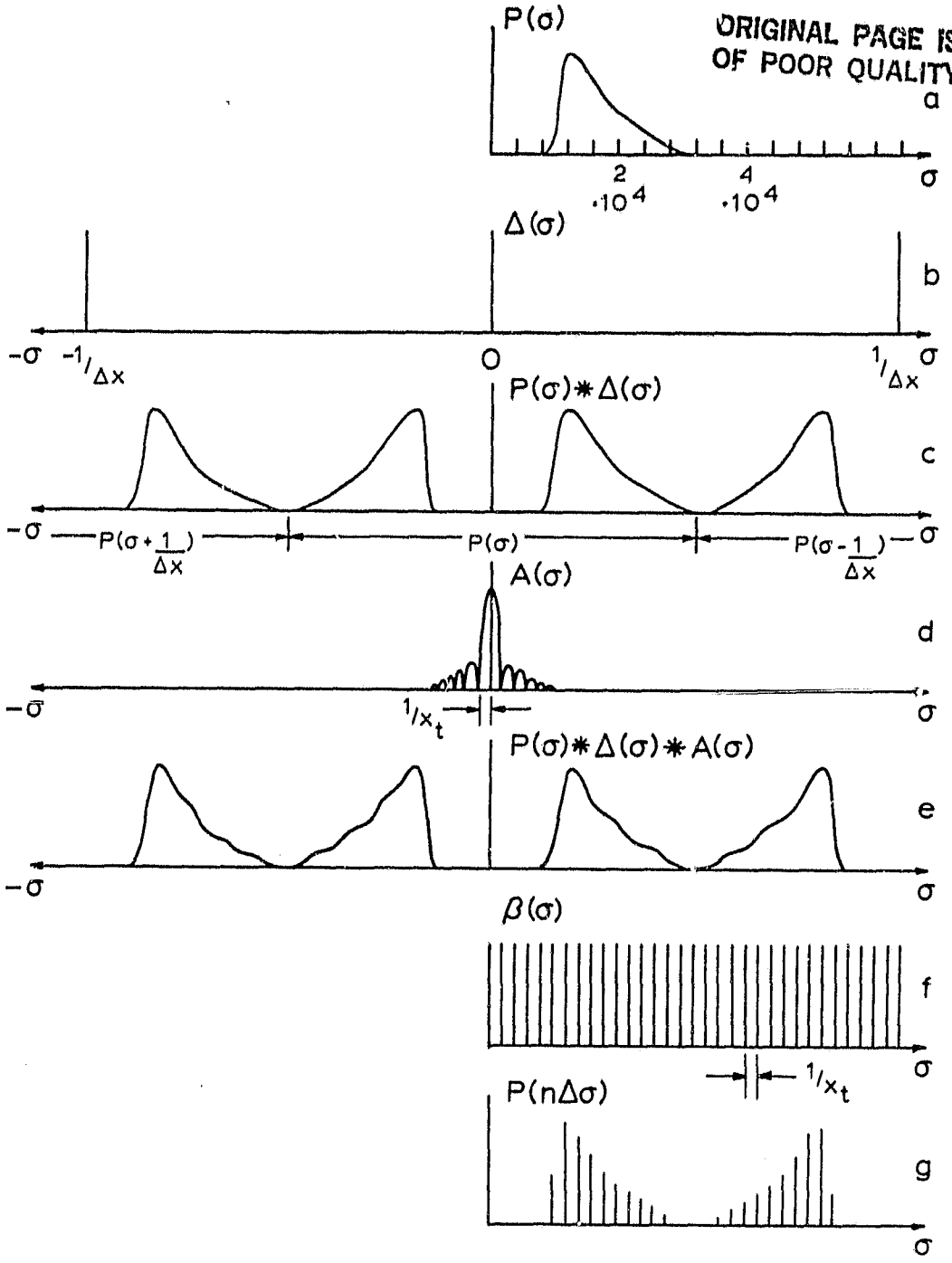

Figure 2. Corresponding signals in the wavenumber, σ, domain. (a) The wavenumber spectrum of the incoming light which is responsible for the interferogram produced by the spectrometer. (b) The Fourier transform of the sampling trigger sequence. In this domain, the delta functions are separated by the reciprocal of the sampling interval in wavenumber units. (c) The convolution of the spectrum with the sampling function. (d) The Fourier transform of the apodization function. (e) The convolution of (a), (b), and (d). (f) The sequence of sampling triggers applied by the discrete Fourier transform to the output. (g) The sampled output spectrum which has a resolution given by the reciprocal of the total path difference displacement.

$$\tilde{\gamma}(x) = \gamma(x)\Delta(x)A(x) = \sum_{k=-\frac{N}{2}}^{\left(\frac{N}{2}\right)-1} \gamma(x)\delta(x-k\Delta x) \tag{7}$$

where $N = \frac{X_T}{\Delta x}$.

Fourier Transformation

In Appendices A, B and C, there are appropriate derivations leading to a formulation of the discrete Fourier transform. When (7) is operated upon by the transform, the discrete spectrum

$$P(n\Delta\sigma) = \sum_{k=-\frac{N}{2}}^{\left(\frac{N}{2}\right)-1} \gamma(k\Delta x)e^{-i2\pi nk/N} \quad n = 0,1,2\ldots,N-1 \tag{8}$$

is produced. Consisting of N samples (like the input interferogram function), the spectral resolution $\Delta\sigma$ is

$$\Delta\sigma = \frac{1}{X_t} = \frac{1}{N\Delta x} \tag{9}$$

Therefore, the total range covered by the discrete spectrum is

$$\sigma t = N\Delta\sigma = \frac{1}{\Delta x} = 2\sigma max \tag{10}$$

if sampling is done at the Nyquist interval. However, as reported in Appendix C, this band contains the wavenumber samples

$$P(n\Delta\sigma) \quad \text{for } 0 \leq n \leq \frac{N}{2}$$

and the samples

$$P[(N-n)\Delta\sigma] = P(-n\Delta\sigma) \text{ for } \frac{N}{2} \leq n \leq N$$

The actual spectrum is of course real only for positive wavenumbers. The spectrum recovered by the transform in the second half of the wavenumber span is the image of the spectrum into negative wavenumbers because of the convolution shown in Figures 2a-c. It is a copy of the real spectrum and does not contain any information. All of the information of importance is contained in the first $\frac{N}{2}$ samples produced by the transform.

OTHER CONSIDERATIONS

In this section several complications must be discussed that impact the operating characteristics of the spectrometer. These include the techniques employed to produce samples evenly spaced in path difference, the errors resulting from imperfections in this technique, and a discussion of the aliasing phenomenon.

Path Difference Sampling Technique

For UVIS, the interference pattern produced by the interferometer is sampled at fixed intervals of time using triggers produced by an external pulse generator. To get measurements of path difference, x, the spectrometer is also used to produce the interference pattern for an incoming He-Ne laser beam. Being a coherent signal, the interference pattern is a sinusoid that does not decay in amplitude as path difference is increased away from ZPD. And, since it is a monochromatic light source, the wavelength of its interference pattern must be equal to its electromagnetic wavelength. This sinusoidal signal is then sampled at the same rate using the external pulse triggers. This rate must be sufficient to enable the accurate calculation of the location of some feature of the sinusoid that can be used to monitor path difference. For UVIS, the zero-crossings were selected as that feature. After subtracting any bias present, the samples are used to compute the zero-crossings by means of a linear interpolation algorithm. If this could be done perfectly then as each zero-crossing was reached during the production of an interferogram, it would be known that .3164 μm of path difference had been traversed. To determine the zero-crossing location to high accuracy requires a high number of pulse generator triggers per interferogram fringe. Both the interval between triggers,

PD, and the period of the fringe pattern are based on time and can be related. The movement of the fringe pattern with time depends only on the axial deformation of the heated aluminum bar as described in PGW. If a voltage is applied to the coil surrounding the bar such that its length changes by HR μm/msec, then the number of msec per zero-crossing is given by .3164/HR. Subsequent division of this by PD msec/samples yields the number of samples per zero crossing, R. Mathematically,

$$R = .3164/(PD \cdot HR) \tag{11}$$

PD and HR must be chosen so that sufficient samples are collected per zero-crossing to ensure that the zero-crossing locations are determined with minimum error.

To explore this further, a sinusoid was sampled by use of a computer program for a range of values of R. Figures 3, 4, 5, 6 and 7 show the error between the interpolated locations of 125 consecutive zero-crossings and the actual locations for R equal to approximately 6, 3, 2, 1.5, and 1.2 samples per zero-crossing, respectively. The maximum error in μm can be selected to characterize the effects of the sampling process. In

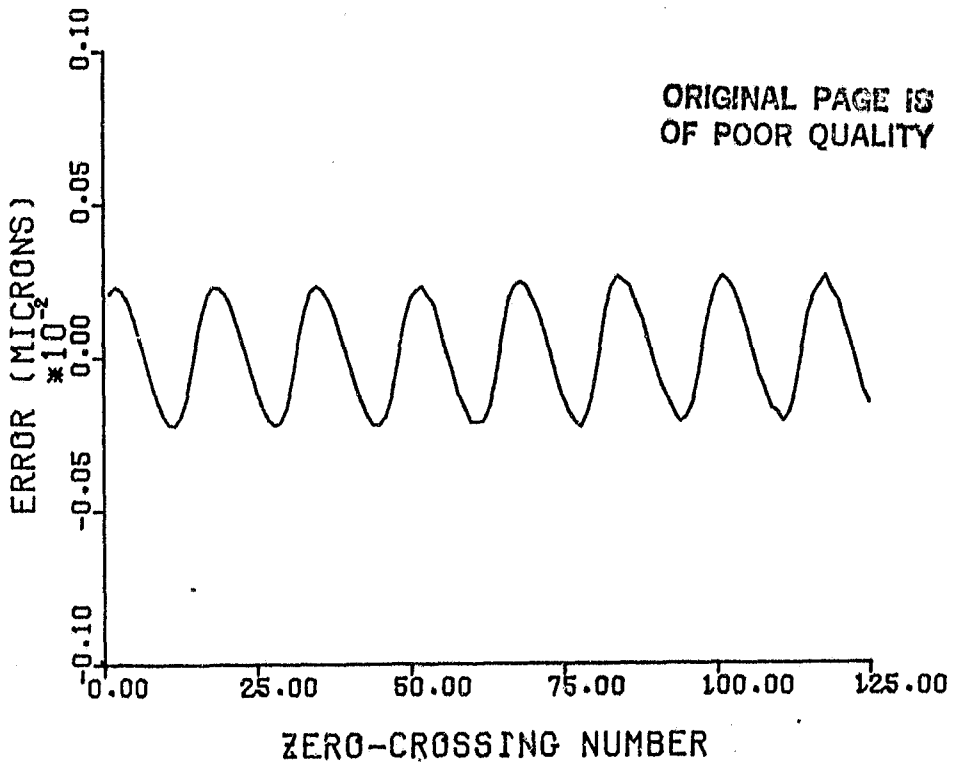

Figure 3. The error in microns resulting from locating the zero-crossings in the laser reference interferogram with a linear interpolator and a sampling rate of six equal time spacing samples per zero-crossing.

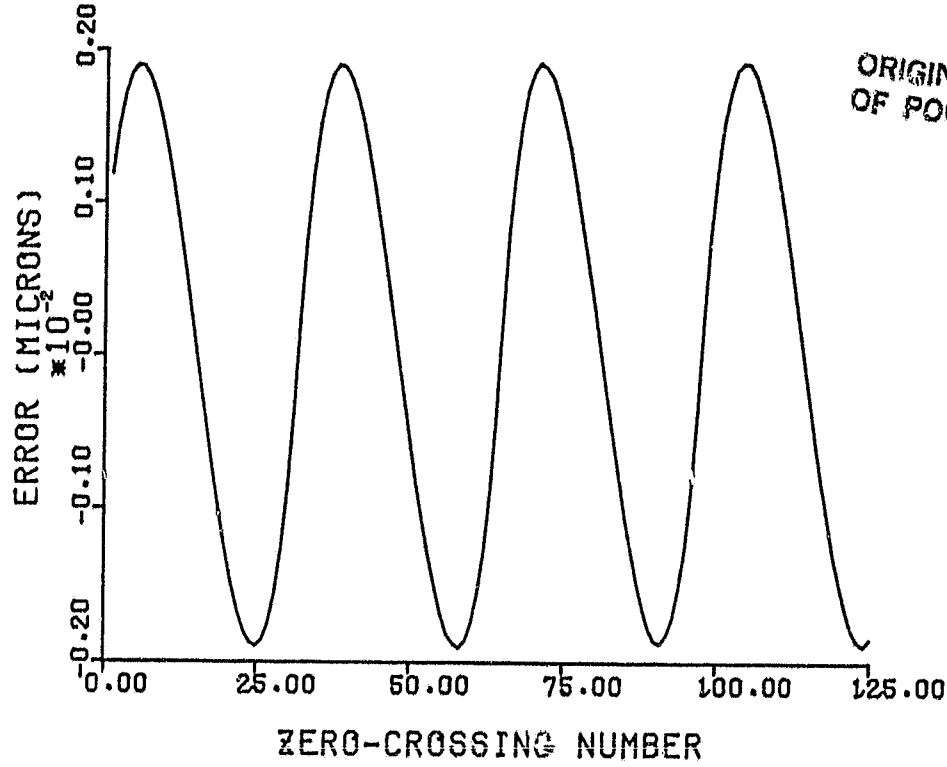

Figure 4. Same as Figure 3 but with three samples per zero-crossing.

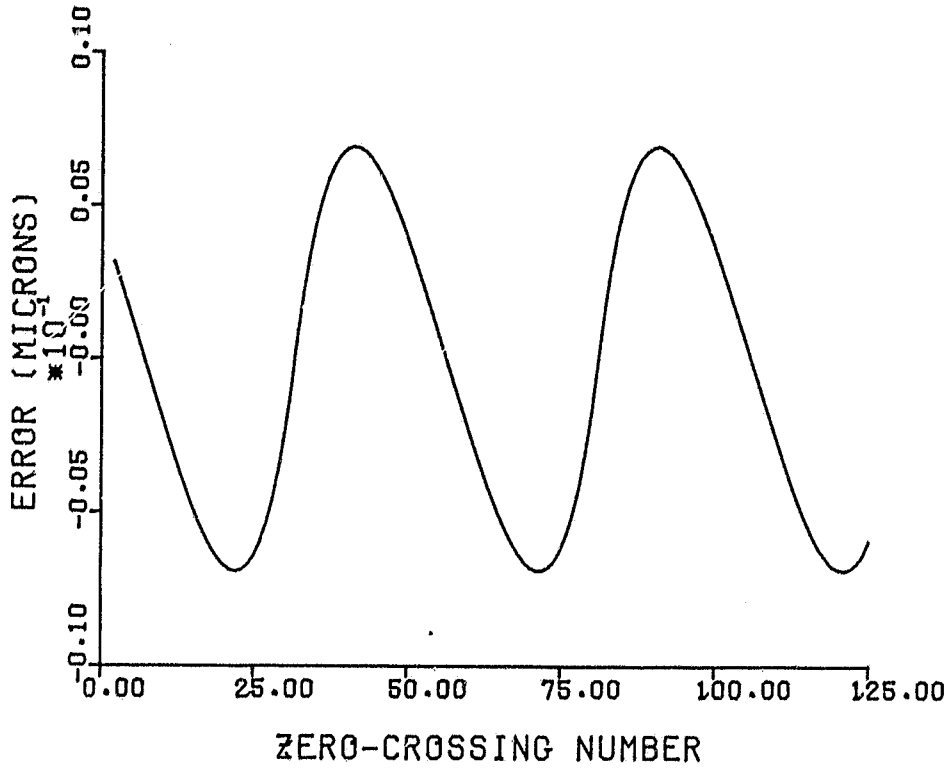

Figure 5. Same as Figure 3 but with two samples per zero-crossing.

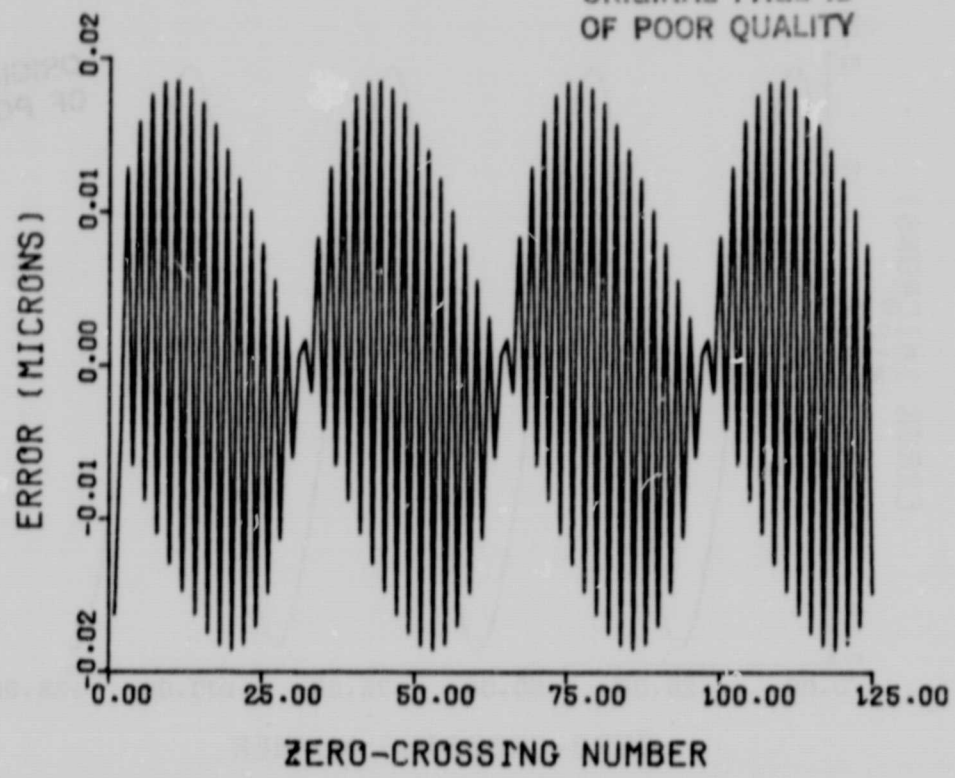

Figure 6. Same as Figure 3 but with 1.5 samples per zero-crossing.

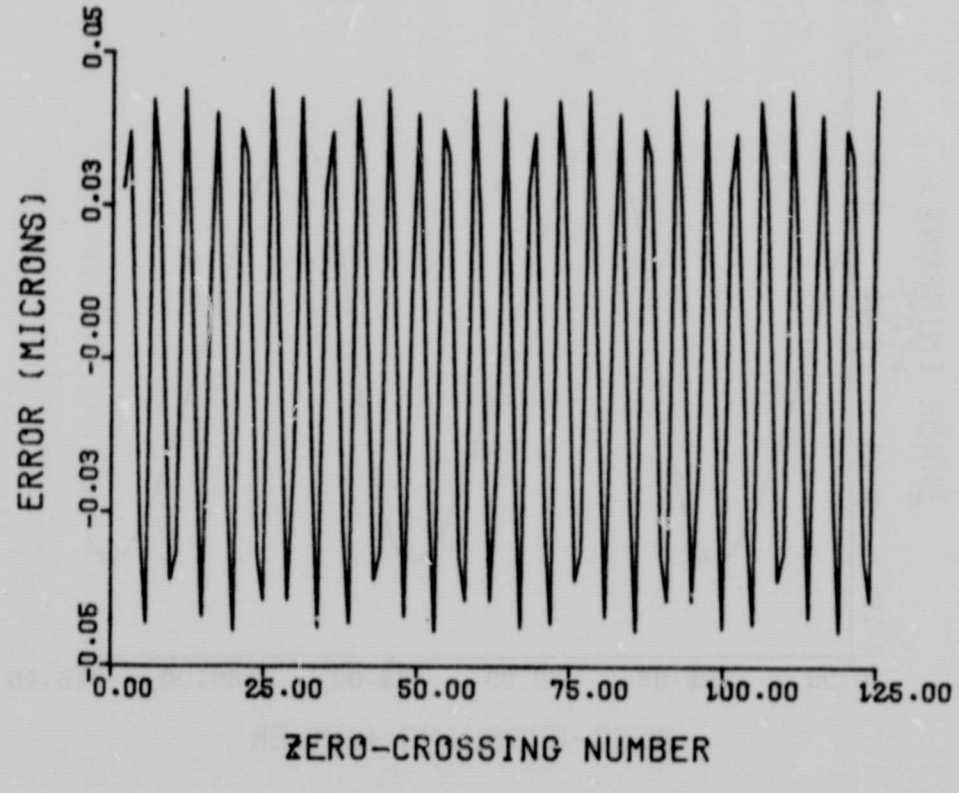

Figure 7. Same as Figure 3 but with 1.2 samples per zero-crossing.

Figure 8, this parameter is plotted versus R. Also, the graph contains the ratio of the maximum error to the zero-crossing separation distance plotted versus R. For example, at a sampling rate of 1.5 samples per zero-crossing, the maximum error is about $1.85 \cdot 10^{-2}$ μm, which is about 5.9% of the zero-crossing spacing.

As discussed in PGW, the zero-crossings are used to determine the approximate values of the interference pattern produced by the solar signal. These constant path difference samples would be unaffected by low frequency changes in the bar heating rate and also would be in the appropriate x domain for transformation by the discrete Fourier transform algorithm. The true cost of the location error discussed above cannot be determined without using these mislocated zero-crossings to trigger the sampling of the solar signal interferogram. To simulate this, the following Fourier transformation relationship can be derived and conveniently used. If

$$P(\sigma) = e^{-\pi^2(\sigma-\sigma_0)^2\tau^2} \cdot \sqrt{\pi}\,\tau \tag{12}$$

where σ_0 is the wavenumber of this Gaussian function's peak value, then

$$\gamma(x) = \frac{1}{2} e^{-x^2/\tau^2} \cos 2\pi\sigma_0 x \tag{13}$$

with

$$\tau = 1/\pi(\sigma'-\sigma_0)$$

σ' is defined to be the wavenumber at which the Gaussian function's amplitude is 1/e of its peak value. The path differences, x, are in microns. If (13) is sampled at the zero-crossing points determined from a linear interpolator and which therefore are mislocated, then a set of samples is produced which is useful for this evaluation. When used as the input data to the Fourier transform algorithm, the function shown in Figure 9 was produced. The solid line represents the original spectrum given by (12) with σ_0 = 11,500 cm^{-1} and σ' = 11,000 cm^{-1}. The errors introduced into this sampling and transformation procedure are those illustrated in Figure 6. This case, which has a maximum mislocation error of $1.85 \cdot 10^{-2}$ μm, results in a recovered spectrum that is most marked by the introduction of a non-negligible artifact at about 4,350 cm^{-1}. Within the skirts of the recovered Gaussian, there is a small shift towards higher wavenumbers as well. The impact of these spectral errors will be discussed later in this section.

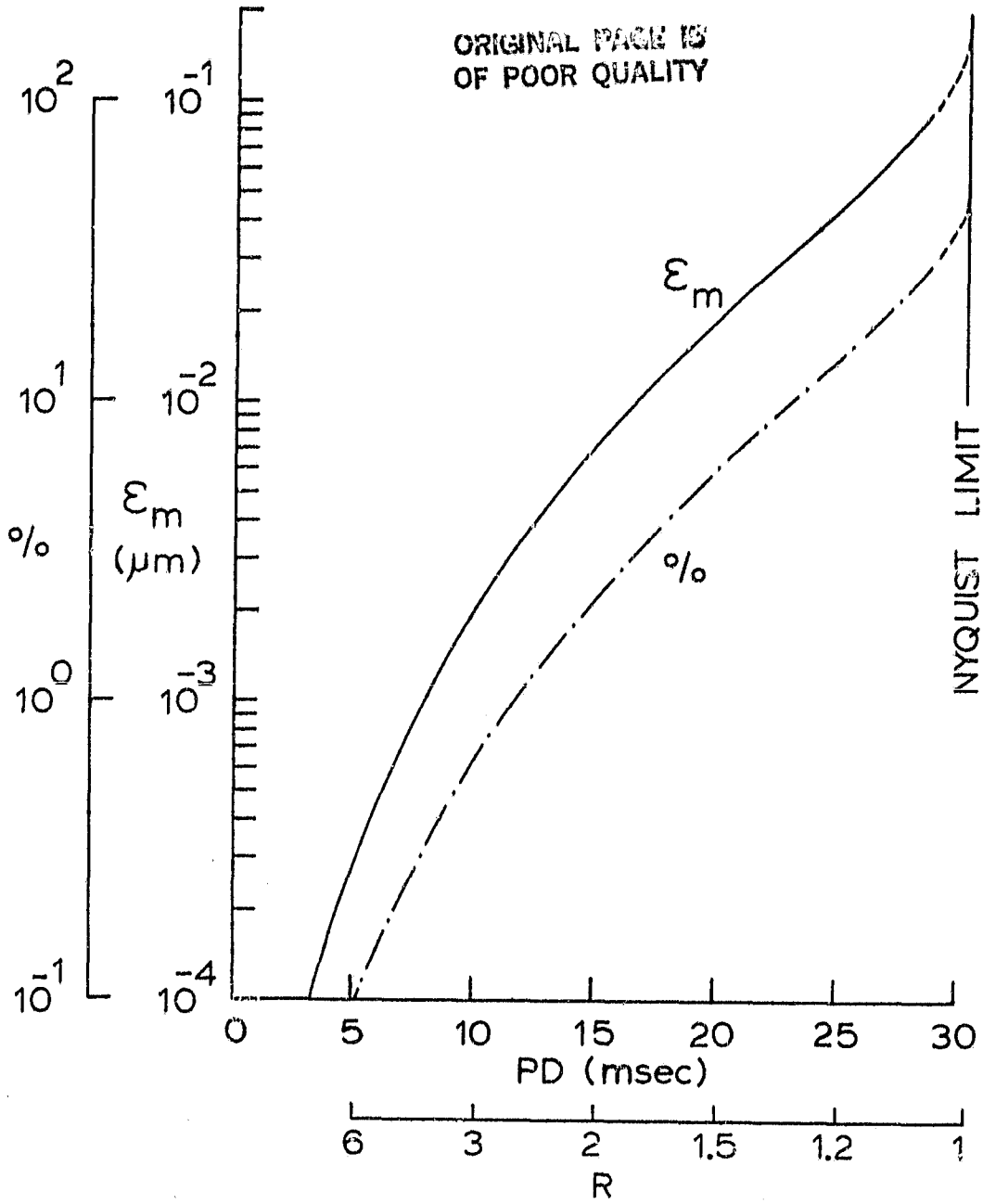

Figure 8. The variation of the maximum zero-crossing mislocation error in microns with the time interval between sampling triggers, PD, in msec. The additional axes show the variation of this error as a percentage of the laser reference zero-crossing path difference .3164 μm as a function of the number of samples per zero-crossing, R.

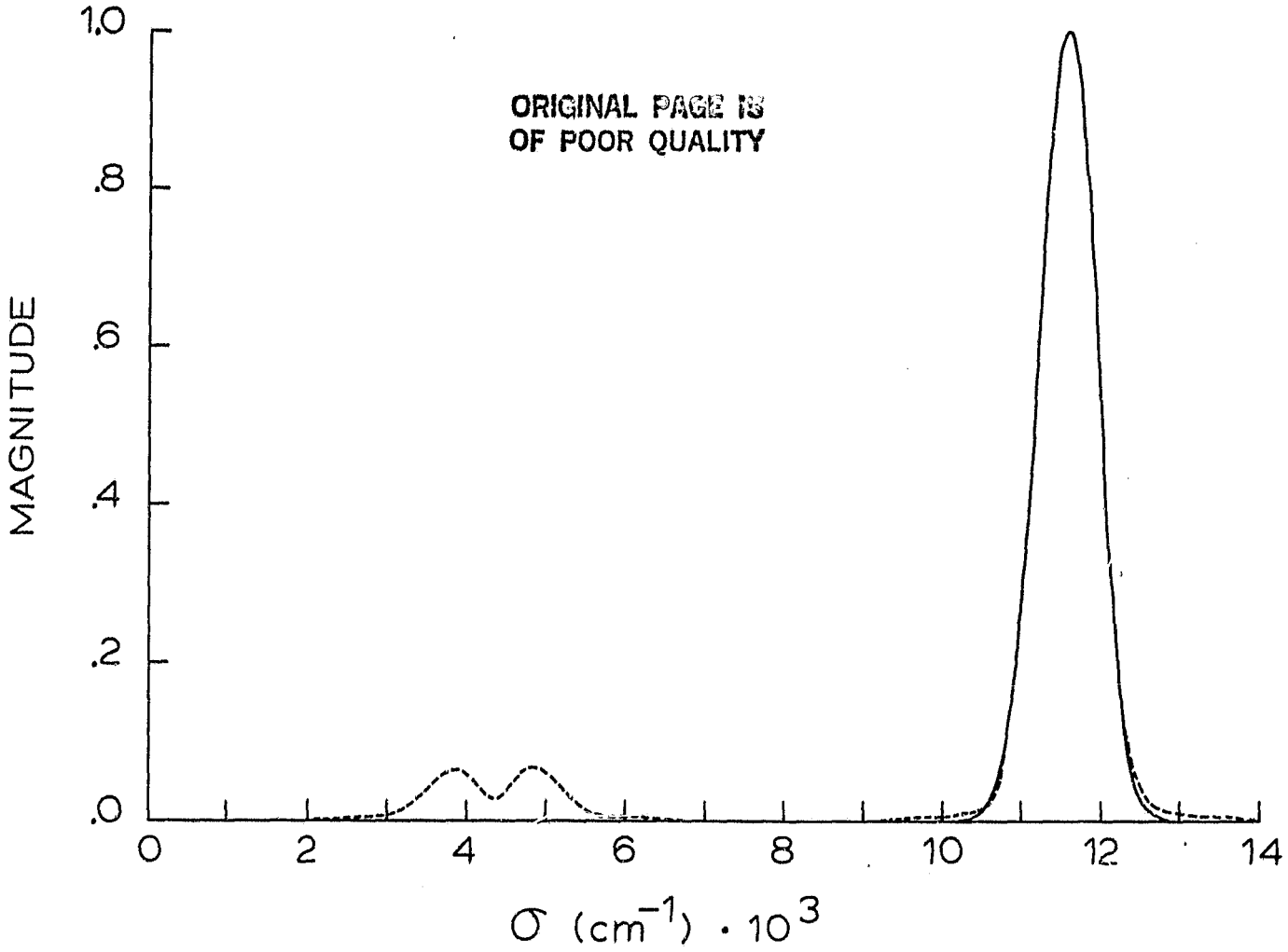

Figure 9. A normalized spectrum produced by the FFT with (-----) and without (———) the interferogram samples being mislocated by the errors plotted in Figure 6.

Interferogram Centering

The only mechanism that has been found to be capable of smoothly moving the interferometer optics by the small path difference required for visible and near-ultraviolet spectral measurements is the heated rod. One might suspect that this technique would be flawed because of inordinate amounts of time that would be required for the bar to be heated and cooled through the appropriate temperature range. With aluminum as the selected material, this is not the case. For a reasonable voltage, the Nichrome heating coil can easily create a bar expansion rate for heating of around 10 μm/sec. A cooling rate nearly as fast can be produced by using an auxiliary fan. If, for example, a spectral resolution of 100 cm^{-1} were desired, then from (9), X_t equals 100 μm. For the above expansion rate, a complete scan can be obtained in about 10 sec. For this length of time, the atmosphere can certainly be considered steady-state.

However, the true cost of the heated bar technique is the lack of registration. Consecutive scans cannot be started at the same path difference. By use of mechanical stops, they can be started within a few microns of the same path difference. Therefore, it is necessary to collect more samples triggered from the pulse generator than are actually needed for the interferogram. By starting a little in advance of the desired scan starting point and by finishing a little beyond the desired end point, there will be a cushion of samples that can be discarded as needed to bring an interferogram into proper registration. If M is the number of pulse generator triggers and if ΔM is the additional samples in the cushion, then the number of zero crossings is given by $(M+\Delta M)/R$. The situation can be further complicated if a path difference sampling interval Δx different from the zero-crossing interval is desired. This can be done in the software by linear interpolation between zero-crossings or by skipping integer numbers of zero-crossings. If the number of final, or constant path difference samples per zero-crossing is K, then the total number of interferogram samples is

$$(N+\Delta N) = (M+\Delta M) \cdot \frac{1}{R} \cdot K \tag{14}$$

where ΔN is the additional numbers of constant path difference samples that is produced by the ΔM samples in the cushion. Zero path difference is found by visual inspection of the final interferogram. Then the ends are truncated as required to produce the proper interferogram length.

Of course, the interpolation and the imprecise determination of zero path difference give rise to potentially important phase errors. It is for this reason that the two-sided interferogram and discrete Fourier transform are used in UVIS. By taking the magnitude of the computed spectrum, these phase errors can be avoided. Consider the following explanation. $P_e(\sigma)$ is the actual spectrum which is even (i.e., symmetrical about ZPD). $\phi(\sigma)$ is the function describing the phase errors present. Then the observed spectrum is

$$P_e(\sigma)e^{-i\phi(\sigma)} = p(\sigma)-iq(\sigma) = \int_{-\infty}^{\infty} \gamma(x)e^{-i2\pi\sigma x}\, dx \tag{15}$$

By taking the magnitude using

$$P_e(\sigma) = \{[p(\sigma)]^2 + [q(\sigma)]^2\}^{1/2} \tag{16}$$

the actual spectrum is recovered regardless of the form of $\phi(\sigma)$.

Aliasing

The final additional consideration that is necessary for describing the operating characteristics of UVIS is aliasing. This phenomenon will be described using Figures 10 and 11, which are modifications of Figures 1 and 2. In Figure 11a, the spectrum from Figure 2a is shown after it has been attenuated on the low wavenumber side in a fashion that is typical of the effects of an optical filter. If its total bandwidth is now less than 1/2 of the upper wavenumber cutoff, σ_{max}, then the benefits of aliasing can be reaped. Figure 10b shows constant path difference sampling performed at twice the interval used in Figure 1b. This results in a replication of the spectrum at intervals of σ_{max}, as shown in Figure 11c. Then, $X_t = N\Delta x$ is twice the total path difference as before, and the spectral resolution is halved as shown in Figure 11f. For the same number of samples, N, the computed spectrum can be found in the first N/2 spectral samples as shown in Figure 11g. The example shown produces a backwards replica of the spectrum because of the wavenumber domain convolution process but this is easily corrected by the software package for UVIS.

The governing equation for aliasing is a modification of (5). If Δx is selected such that

$$\Delta x \leq \frac{1}{2(\sigma_{max}-\sigma_o)} \tag{17}$$

where σ_o is the lower wavenumber cutoff of the filtered spectrum and where

$$\sigma_{max} - \sigma_o = \sigma_{max}/m \tag{18}$$

then aliasing can be a beneficial attribute of the spectral recovery scheme. m is an integer and is called the spectral order. For the example above, m = 2 and $\sigma_o \geq \sigma_{max}/2$.

One specific requirement for this technique to work is that there are <u>no</u> spectral components below σ_o. If there are, then the aliasing will introduce these components as contaminants to the replicated spectrum produced by the convolution. Therefore, the artifact produced by the laser beam interferogram interpolation procedure that is shown in Figure 9 could not be tolerated if aliasing was being used.

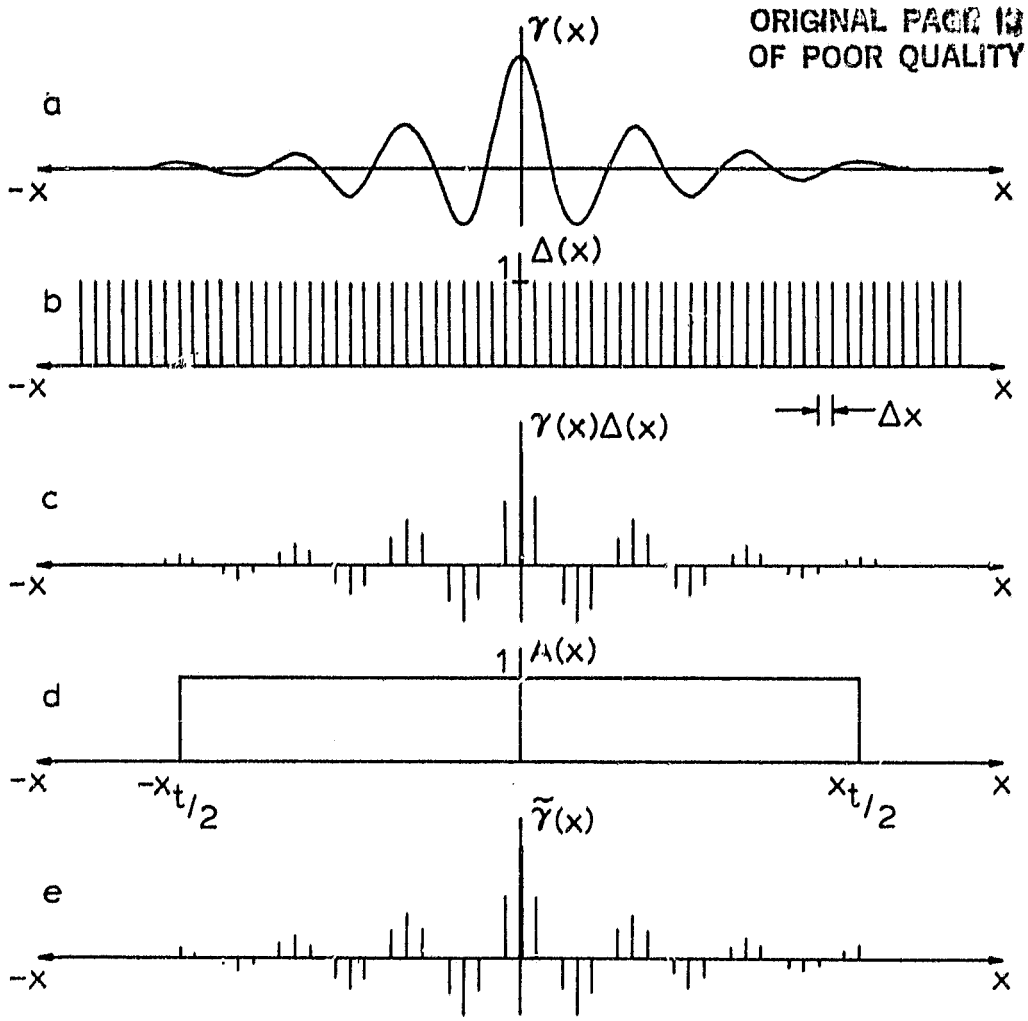

Figure 10. Same as Figure 1 except that the path difference sampling is performed with Δx double that used before.

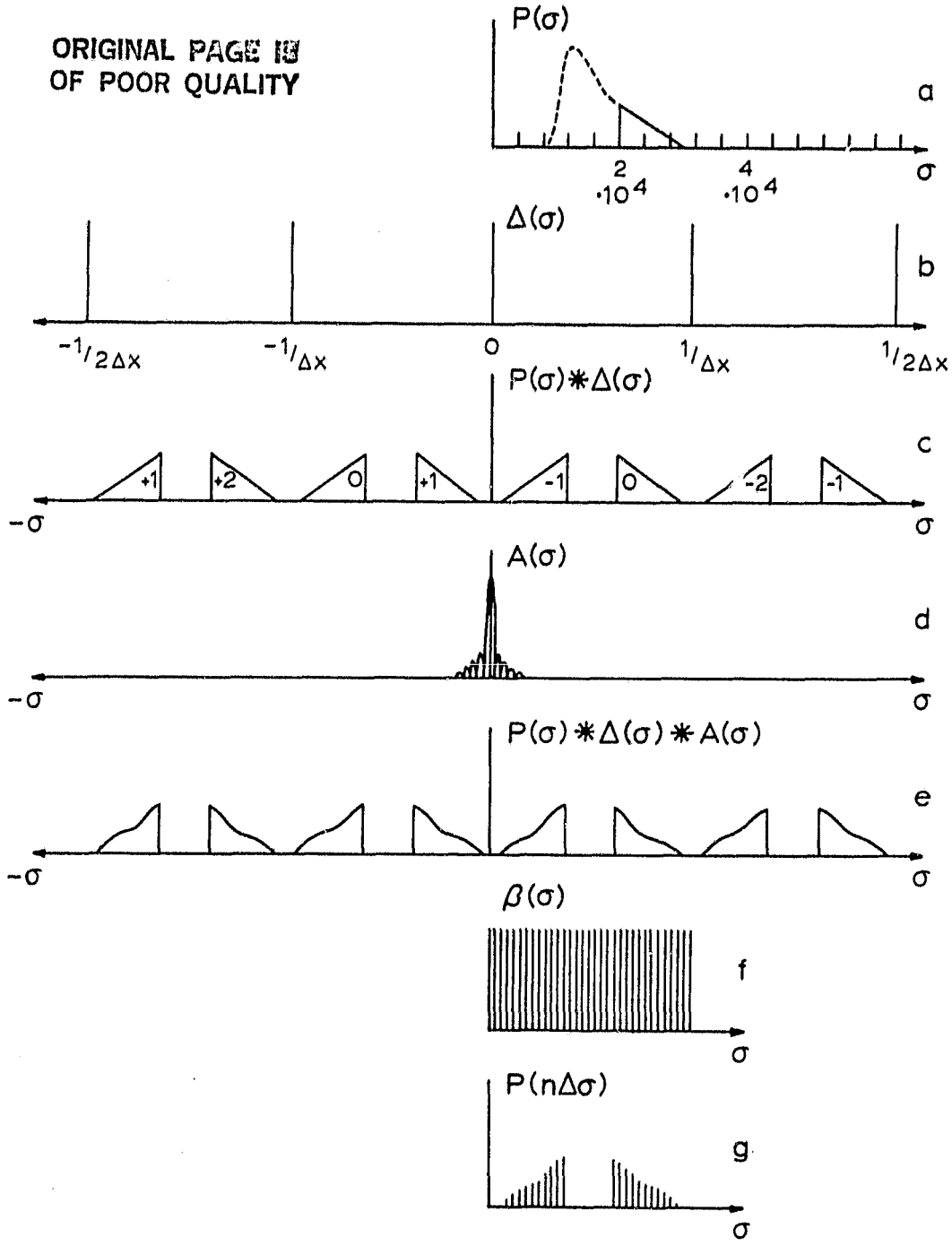

Figure 11. Corresponding signals in the wavenumber, σ, domain. (a) The spectrum of the incoming light is filtered so that the low wavenumber portion is missing. (b) With Δx twice as large as in Figures 1 and 2, the sampling function triggers in the wavenumber domain are spaced half as far apart. (c) The convolution of (a) and (b). (d) The Fourier transform of an apodization function having twice the total path difference displacement as before. (e) The convolution of (a), (b), and (d). (f) The sequence of sampling triggers applied by the FFT to the output. (g) The sampled output spectrum with twice the resolution as in Figure 2 but with the same number of samples because of the use of aliasing.

SYSTEM OPERATING CHARACTERISTICS GOVERNING EQUATIONS

From all of the preceding discussions, a system of equations has been developed which completely describe how an instrument system such as UVIS will operate. These are recapitulated below for review.

$$\Delta x \leq \frac{1}{2(\sigma_{max}-\sigma_o)} \tag{19a}$$

$$m(\sigma_{max}-\sigma_o) = \sigma_{max} \tag{19b}$$

$$N + \Delta N = (M + \Delta M) \cdot \frac{1}{R} \cdot K \tag{19c}$$

$$N = 2^J, \ J \text{ an integer} \tag{19d}$$

$$T_t = (M + \Delta M) \cdot PD \tag{19e}$$

$$X_t = (N + \Delta N)\Delta x \tag{19f}$$

$$\Delta\sigma = \frac{1}{N\Delta x} \tag{19g}$$

$$\sigma t = 2\sigma_{max} \tag{19h}$$

$$R = .3164/(PD \cdot HR) \tag{19i}$$

These have been recombined in a simple computer model to produce values of σ_{max}, m, Δx, K, N, M + ΔM, X_t, and T_t given input values for σ_{max}, σ_{min}, $\Delta\sigma$, PD, HR, and ΔN. An initial value for σ_{max} is entered and the output σ_{max} value produced is the wavenumber needed to satisfy (19a,b,d,g) in combination. The Fortran code for this model is included as Appendix D and is suitable for use with the DEC RT-11 version 3b operating system.

MODEL RESULTS

The following results have been produced using the model subject to these conditions. First, the cushion ΔM has been set at 10% of N. Secondly, the bar expansion rate of 10 μm/sec is fixed. However, the pulse generator triggering rate PD is variable. Based upon the result given in Figure 9, it seems prudent to require that PD be less than 20 msec/sample. This is equivalent to saying that R should be kept greater than 1.5 reference samples per zero-crossing.

One of the input parameters is $\Delta\sigma$, the output spectral resolution. Of course, it would be desirable to keep this as small as possible. In the visible and near-ultraviolet wavelengths, most scientists and engineers tend to use wavelength, λ, as the unit of measurement rather than wavenumber, σ. Therefore, it is important to point out that a constant resolution $\Delta\sigma$ does not correspond to a constant resolution $\Delta\lambda$. The wavelength at which the resolution element $\Delta\sigma$ is located influences the corresponding resolution $\Delta\lambda$. This is illustrated in Figure 12. For example, a resolution of 100 cm^{-1} at 1.0 μm is equivalent to a wavelength resolution of 100Å; but at 0.3 μm, it is equivalent to 9Å. $\Delta\sigma$ = 40 cm^{-1} is the same as 40Å at 1.0 μm and 3.6Å at 0.3 μm. As will be seen in the model results, quite high wavelength resolution in the ultraviolet is possible if sufficient samples can be collected and transformed. As seen in (19g), $\Delta\sigma$ is dependent upon ΔX, the interval of constant path difference. It should be observed that the original sampled data contains higher resolution information because of the requirement that there be enough time samples per zero-crossing to make possible accurate interpolations of the zero-crossing locations. This information is lost, however, because of the FFT algorithm requirement for evenly spaced data points in path differences.

Before specifying the optimum operational characteristics of the UVIS, it is instructive to exercise this model to examine the variability of the important output parameters for a range of input parameter values. Figure 13 shows how M and N vary for a number of σ_{max} values. Only spectral order 1 (m=1) solutions are plotted and the spectral resolution is 40 cm^{-1}. The pulse generator trigger period, PD, is 20 msec. The discontinuities in the curves are the result of the requirement that N is a power of 2. Within each plateau region, the value of K, the number of output samples per zero-crossing, is also given.

In Figure 14, the effects of varying PD is examined for the different spectral resolutions, 100 cm^{-1} and 40 cm^{-1}. Again only solutions for spectral order 1 are shown and σ_{max} is set at 30,000 cm^{-1}; K is constant for all solutions and equal to 2 samples per zero-crossing.

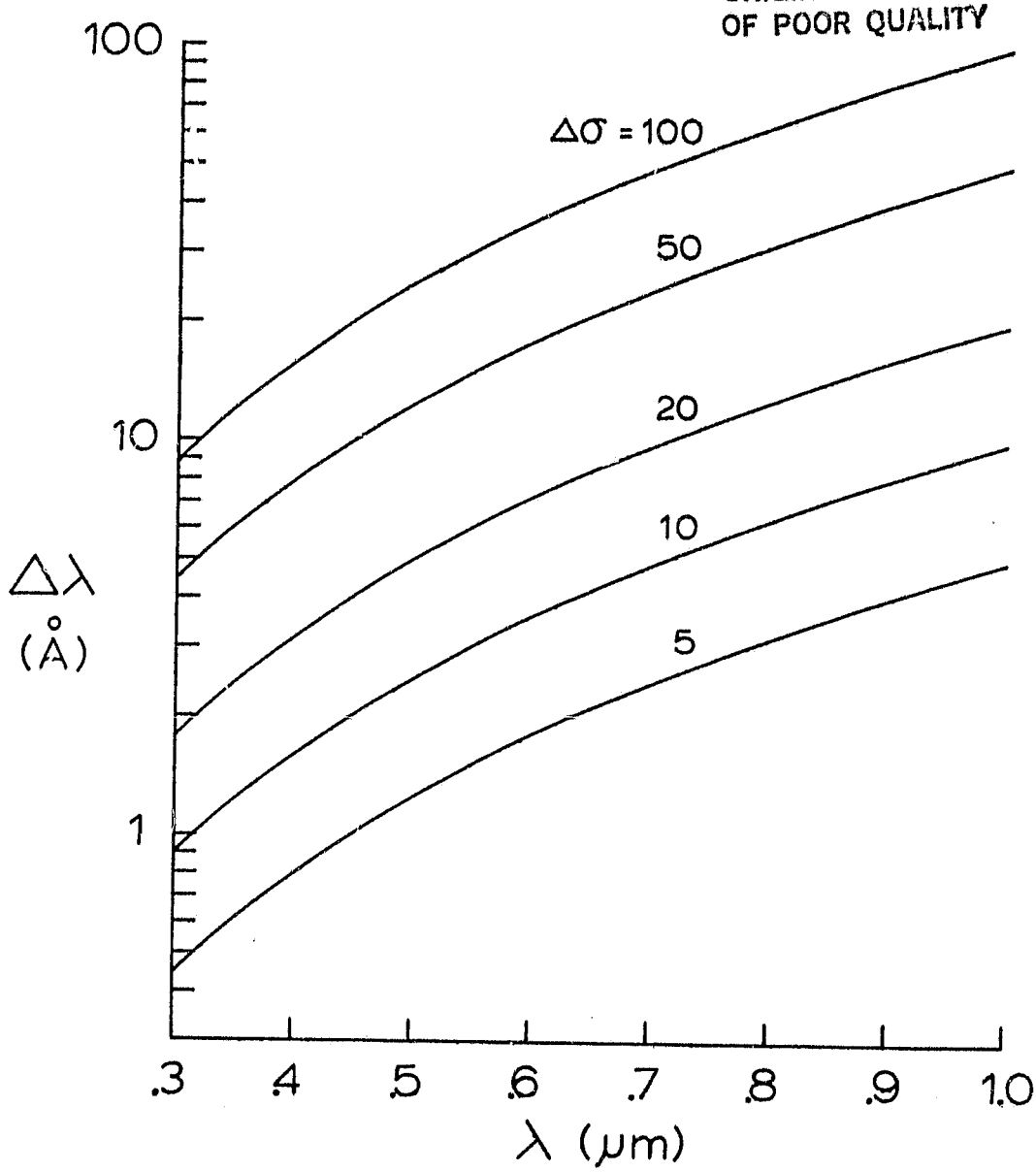

Figure 12. The correspondence between intervals of wavelength in A and intervals of wavenumber in cm^{-1} as a function of wavelength.

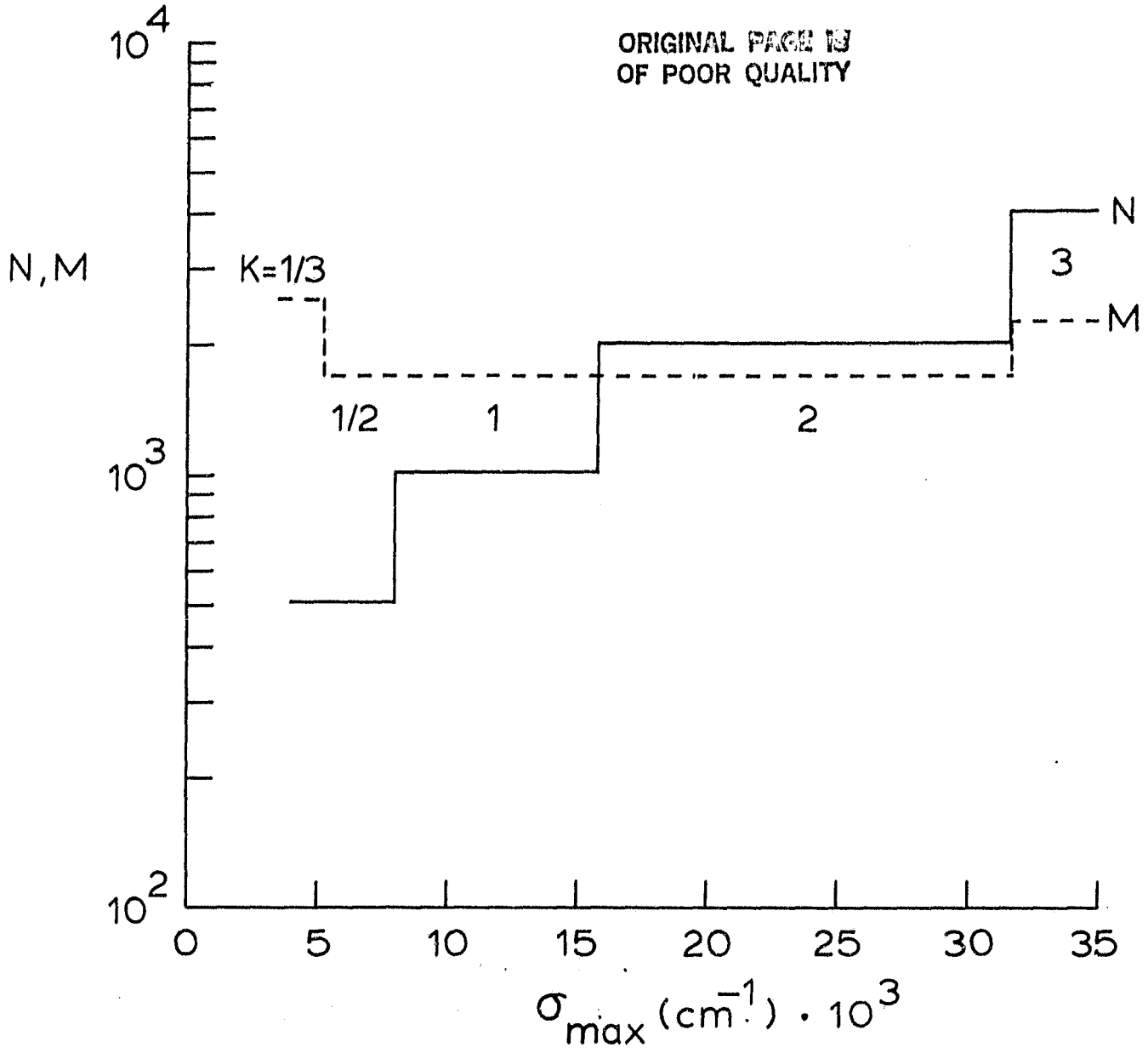

Figure 13. The variation of M and N with maximum wavenumber. Only spectral order 1 solutions at a resolution of 40 cm^{-1} are shown. PD is 20 msec and the number of samples per zero-crossing, K, are shown in-between the discontinuities.

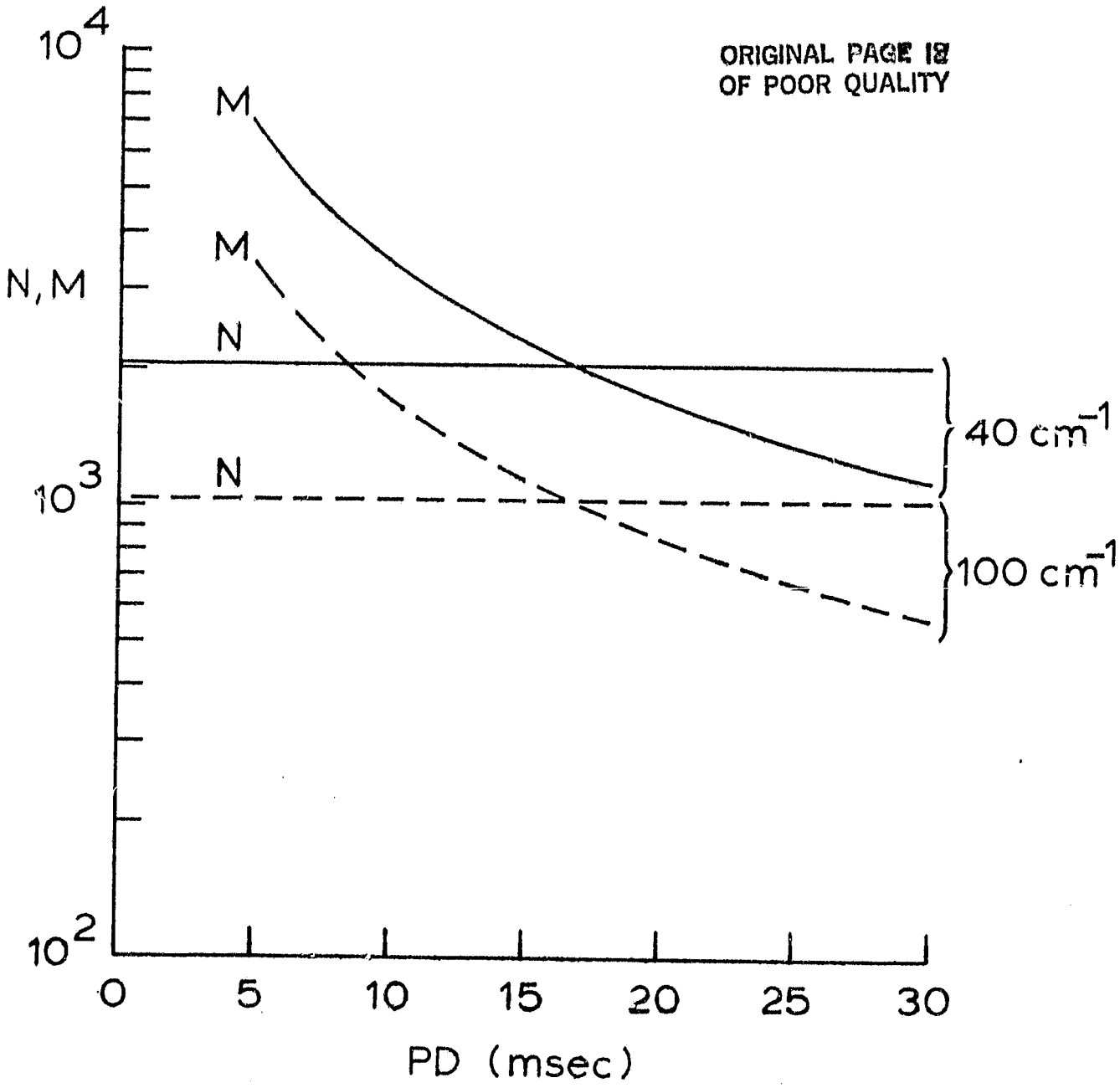

Figure 14. The variation of M and N with PD. Curves for both 40 cm^{-1} and 100 cm^{-1} resolutions are shown.

UVIS OPERATING CONDITIONS

To specifically identify the operating parameter values for UVIS, it is necessary to identify the appropriate values of σ_{max}, σ_o, and $\Delta\sigma$ for potential applications of UVIS. As discussed in PGW, the instrument uses silicon photodiode detectors that are responsive from about .25 μm - 1.1 μm. That is, they are sensitive to radiation from the near ultraviolet through the visible and into the near-infrared. Figure 15 is the solar spectrum plotted against wavenumber as reported by Mecherikunnel (1980). Tentatively, this can be divided into three broadband regions that can be used for the following applications. From about 10,000-15,000 cm^{-1}, there are three water vapor absorption band systems. By monitoring the difference between the signal strength at the center of these bands to the signal level at unattenuated wavenumbers just outside these bands, estimates can be made of the amount of water vapor present in the atmosphere. Preliminary results from UVIS for this application have been reported by Parsons (1983). From 20,000 - 30,000 cm^{-1}, the solar spectrum becomes increasingly attenuated by ozone as the wavenumber increases. By monitoring the gradient of the sun's intensity with wavenumber and hopefully by monitoring its value at specific ozone absorption lines, UVIS may be able to measure total ozone amounts. Finally, the spectral band between 15,000 and 25,000 cm^{-1} encompasses the visible wavelengths and an interferometric spectrometer operating within this band would obviously have many uses.

Therefore, these three bands are adopted for this modelling effort to give reasonable values for σ_{max} and σ_{min}. $\Delta\sigma$ cannot be specified at the desired levels because of computer memory constraints. The LSI-11/02 system used in UVIS has a memory capacity of 32K words of which 28K words are available to the programmer. This limits the value of N to 512 or less and M to 1200 or less. $\Delta\sigma$ will be selected at the highest resolution possible to accommodate this constraint. Figure 14 shows that at $\Delta\sigma$ = 100 cm^{-1}, for example, the required number of original samples, M, rises dramatically for smaller values of PD to produce the same number of final samples, N.

To stay within the memory limit and also to keep PD less than 20 msec to avoid the interpolation artifact problem may necessitate a very narrow range of operating conditions. This is examined in the following illustration. Figure 16 shows the variation of N and M with $\Delta\sigma$ for the bandpass covering 10,000 - 15,000 cm^{-1} and for R = 1.5. This graph shows that for this band, both spectral orders 1 and 2 are usable. Of course, m=1 implies that the resultant spectrum covers the entire range of wavenumbers from 0 cm^{-1} to 15,000 cm^{-1}. Actually σ_{max} is 15,802 cm^{-1}. For m=2, σ_o = 7,901 cm^{-1} instead of 0 cm^{-1}. To conform to the computer memory limit, the maximum resolution that can be achieved for R = 1.5 is 61.73 cm^{-1}. Table I summarizes the information contained in Figure 16 and adds similar information for the same bandpass but for the R = 2.0 and

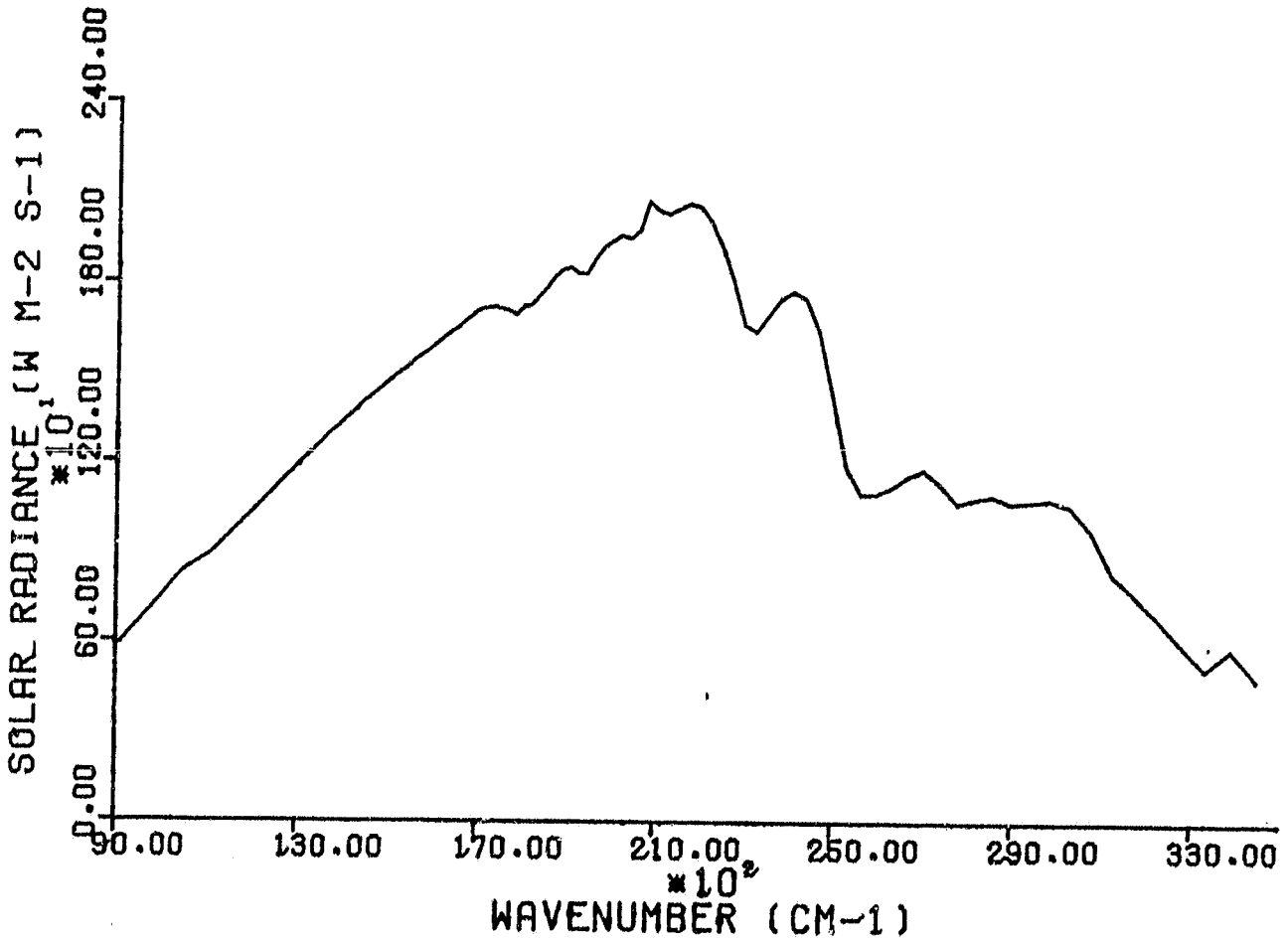

Figure 15. The solar radiance spectrum from Mercherikunnel and Richmond (1980).

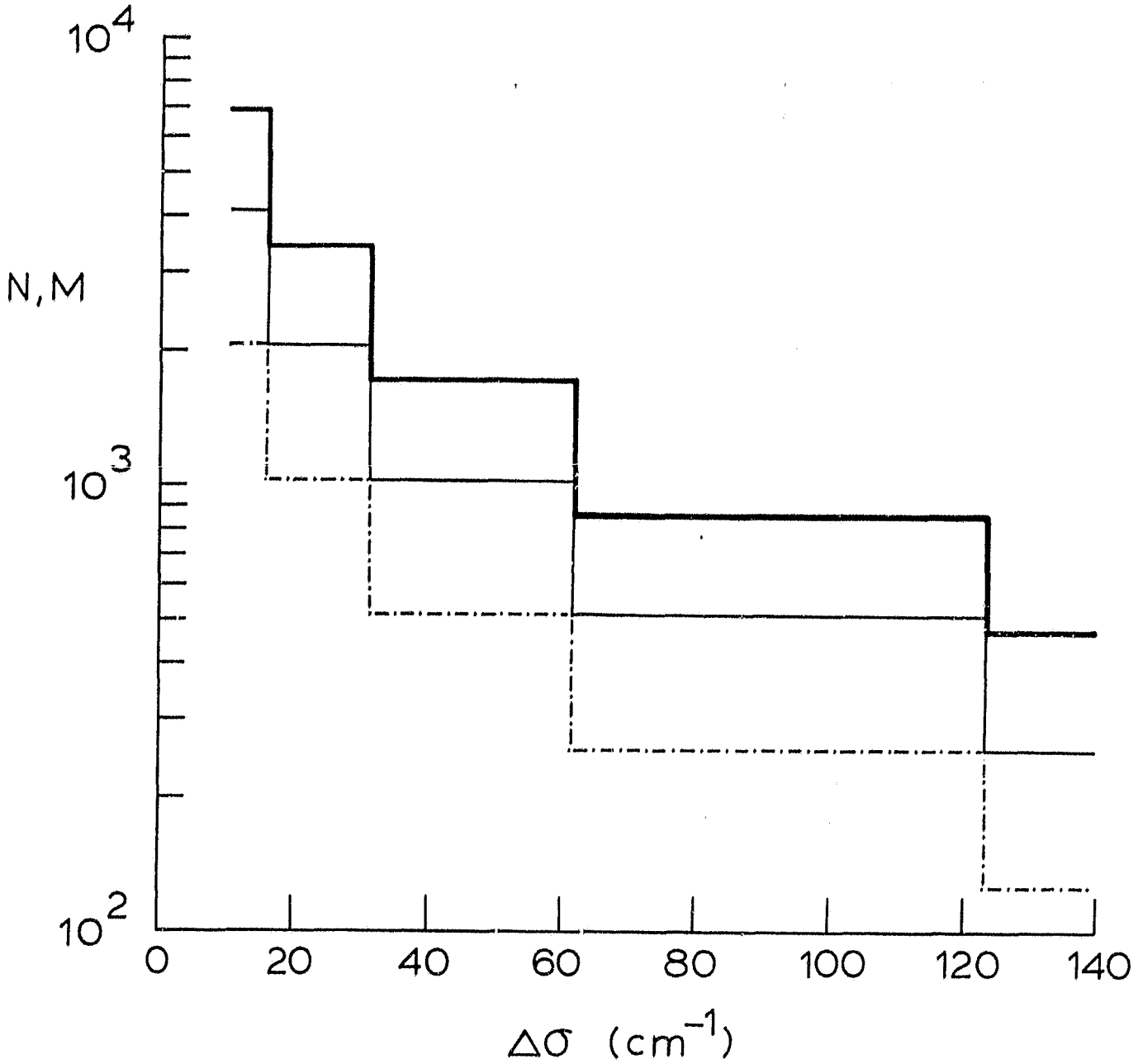

Figure 16. The variation of M and N with spectral resolution for a spectral bandpass of 10,000-15,000 cm^{-1} and 1.5 samples per zero-crossing. ——, M; ——, N (spectral order 1, K=1); —·—·—, N (spectral order 2, K=1/2).

R = 3.0 cases. For R = 3.0, it indicates that 123.46 cm^{-1} is the maximum resolution achievable.

Table II applies to the ultraviolet bandpass containing the ozone absorption features. For sampling rates of 1.5 and 2.0 final samples per zero-crossing $\Delta\sigma$ = 61.73 cm^{-1} is possible but only for spectral order 2. For R = 3.0, again only 123.40 cm^{-1} resolution is achievable. Finally, the visible wavelength bandpass is studied in Table III. For $\sigma_{max} \cong 25{,}000$ cm^{-1} and $\sigma_0 \cong 15{,}000$ cm^{-1}, the possibility of using aliasing and spectral order 2 is gone. Unfortunately, for all three sampling rates the best resolution possible is 123.46 cm^{-1}.

To summarize these findings Table IV is presented. It contains the pertinent information from these model results. When several operating modes are possible, the one with the best resolution and the highest sampling rate R is the one entered in the table. The information entered for the 15,000 - 25,000 cm^{-1} case is also appropriate if the entire spectrum to 30,000 cm^{-1} is to be recovered.

TABLE I. SAMPLING REQUIREMENTS FOR WAVENUMBER REGION 8000-15000 cm^{-1}

$\Delta\sigma$ Range (cm^{-1})	N		M		
	m=1	m=2	R=1.5	R=2.0	R=3.0
15.43 - 30.87	2048	1024	3414	4549	6824
30.87 - 61.73	1024	512	1704	2276	3414
61.73 - 123.46	512	256	854	1136	1704
123.46 - 246.92	256	128	426	569	854

TABLE II. SAMPLING REQUIREMENTS FOR WAVENUMBER REGION 20000-30000 cm^{-1}

$\Delta\sigma$ Range (cm^{-1})	N		M		
	m=1	m=2	R=1.5	R=2.0	R=3.0
15.43 - 30.87	4096	2048	3414	4549	6824
30.87 - 61.73	2048	1024	1706	2276	3414
61.73 - 123.46	1024	512	854	1136	1704
123.46 - 246.92	512	256	426	569	854

TABLE III. SAMPLING REQUIREMENTS FOR WAVENUMBER REGION 15000-25000 cm^{-1}

$\Delta\sigma$ Range (cm^{-1})	N		M		
	m=1	m=2	R=1.5	R=2.0	R=3.0
15.43 - 30.87	4096	3414	4551	4551	6827
30.87 - 61.73	2048	1706	2274	2274	3412
61.73 - 123.46	1024	854	1138	1138	1707
123.46 - 246.92	512	426	568	568	852

TABLE IV. SUMMARY OF OPTIMUM OPERATING CHARACTERISTICS IN ALL THREE BANDS.

	σ band 10-15,00 cm^{-1}	σ band 15-25,000 cm^{-1}	σ band 20-30,000 cm^{-1}
N	512	512	512
M	1137	851	1137
$\Delta\sigma$	61.73 cm^{-1}	123.46 cm^{-1}	61.73 cm^{-1}
R	2.0	3.0	2.0
m	1.0	1.0	2.0
Δx	.3164 μm	.1582 μm	.3164 μm
X_t	.3593 mm	.1347 mm	.3593 mm
T_t	17.033 sec	8.5167 sec	17.033 sec
σ_{max}	15802.78 cm^{-1}	31605.57 cm^{-1}	31605.56 cm^{-1}
σ_o	0.0 cm^{-1}	0.0 cm^{-1}	15802.78 cm^{-1}
PD	15.0 msec	10.0 msec	15.0 msec

CONCLUSIONS

Using the design of the ultraviolet interferometric spectrometer (UVIS) and the fundamentals of the discrete Fourier transform, the optimum operating characteristics of the instrument have been developed for three broadband spectral regions. Each of these regions contains the signatures of atmospheric constituents which are important to several applications.

REFERENCES

Chamberlain, J. (1979), The Principles of Interferometric Spectroscopy, John Wiley & Sons, New York, 347 pp.

Mecherikunnel, A. T., and J. C. Richmond (1980), Spectral Distribution of Solar Radiation, NASA Technical Memorandum 82021, 86 pp.

Parsons, C. L. (1983), "A Fourier Transform Spectrometer for Measurements of Atmospheric Extinction Between 0.4-1.0 μm," presented at WMO/AMS/CMOS Fifth Symposium on Meteorological Observations and Instrumentation, April 11-15, Toronto, Ontario, Canada.

Parsons, C. L., J. C. Gerlach, and M. Whitehurst (1982), A Fourier Transform Spectrometer for Visible and Near-Ultraviolet Measurements of Atmospheric Absorption, NASA Technical Memorandum 73297, 20 pp.

APPENDIX A

THE FOURIER TRANSFORM OF A GENERAL PERIODIC FUNCTION f(x)

From Appendix B, it is seen that

$$F\{1\} = \delta(\sigma)$$

One of the useful general properties of the Fourier Transform is frequency shifting or modulation. Mathematically, this is evident as the following derivation illustrates.

$$F\{e^{i2\pi\sigma_0 x} f(x)\} = \int_{-\infty}^{\infty} f(x)e^{-i2\pi(\sigma-\sigma_0)x}\,dx$$

$$= f'(\sigma-\sigma_0)$$

where f' is the Fourier transform of f. If f(x) is the constant 1, then

$$F\{e^{i2\pi\sigma_0 x}\} = \delta(\sigma-\sigma_0)$$

This can be usefully applied to the following expression

$$f(x) = \sum_{n=-\infty}^{\infty} \alpha_n e^{i2\pi\left(\frac{n}{x_0}\right)x}$$

which states that any periodic function can be represented as the infinite sum of complex sinusoids weighted by coefficients given by

$$\alpha_n = \frac{1}{x_0}\int_{-x_0/2}^{x_0/2} f(x)e^{-i2\pi\left(\frac{n}{x_0}\right)x}\,dx$$

Using the Fourier transform definition,

$$F\{f(x)\} = \int_{-\infty}^{\infty} \left[\sum_{n=-\infty}^{\infty} \alpha_n e^{i2\pi\left(\frac{n}{x_0}\right)x} \right] e^{-i2\pi\sigma x} \, dx$$

$$= \sum_{n=-\infty}^{\infty} \alpha_n \int_{-\infty}^{\infty} e^{i2\pi\left(\frac{n}{x_0}\right)x} \, e^{-i2\pi\sigma x} \, dx$$

Using the frequency shift property,

$$F\{f(x)\} = \sum_{n=-\infty}^{\infty} \alpha_n \, \delta\left(\sigma - \frac{n}{x_0}\right)$$

APPENDIX B

THE FOURIER TRANSFORM OF A CONSTANT

Using $e^{-\eta|x|}$ as a convergence factor,

$$F\{1\} = \lim_{\eta\to 0} \int_{-\infty}^{\infty} e^{-\eta|x|}\, e^{-i2\pi\sigma x}\, dx$$

$$= \lim_{\eta\to 0} \left[\int_{-\infty}^{0} e^{(\eta - i2\pi\sigma)x}\, dx + \int_{0}^{\infty} e^{-(\eta + i2\pi\sigma)x}\, dx \right]$$

$$= \lim_{\eta\to 0} \left[\frac{\exp(\eta - i2\pi\sigma)x}{\eta - i2\pi\sigma} \Bigg|_{-\infty}^{0} - \frac{\exp(-(\eta + i2\pi\sigma)x)}{\eta + i2\pi\sigma} \Bigg|_{0}^{\infty} \right]$$

$$= \lim_{\eta\to 0} \left[\frac{1}{\eta - i2\pi\sigma} + \frac{1}{\eta + i2\pi\sigma} \right]$$

$$= \lim_{\eta\to 0} \left[\frac{\eta + i2\pi\sigma + \eta - i2\pi\sigma}{\eta^2 + (2\pi\sigma)^2} \right] = \lim_{\eta\to 0} \left[\frac{2\eta}{\eta^2 + (2\pi\sigma)^2} \right]$$

In the limit, there is a singularity at $\sigma = 0$. By invoking L'Hospital's Rule, the limit can be evaluated, however, and found to be

$$F\{1\} = \lim_{\eta\to 0} \left(\frac{2}{2\eta}\right)$$

$$= \begin{cases} \infty & \text{at } \sigma = 0 \\ 0 & \text{at } \sigma \neq 0 \end{cases}$$

The area under the function can be obtained from

$$\int_{-\infty}^{\infty} \frac{2\eta}{\eta^2+(2\pi\sigma)^2}\, d\sigma = \int_{-\infty}^{\infty} \frac{2\eta}{\eta^2+w^2}\, \frac{dw}{2\pi}$$

where $w = 2\pi\sigma$ has been used as a substitution. Proceeding,

$$\int_{-\infty}^{\infty} \frac{2\eta}{\eta^2+w^2}\, \frac{dw}{2\pi} = \int_{\infty}^{\infty} \frac{2\eta}{\eta^2\left(1+\frac{w^2}{\eta^2}\right)}\, \frac{dw}{2\pi}$$

$$= \frac{1}{\eta\pi} \int_{-\infty}^{\infty} \frac{dw}{1+\frac{w^2}{\eta^2}} = \frac{1}{\eta\pi} \int_{-\infty}^{\infty} \frac{\eta dx}{1+x^2}$$

using $x = \frac{w}{\eta}$ as a substitution. Then,

$$\frac{1}{\pi} \int_{-\infty}^{\infty} \frac{dx}{1+x^2} = \frac{1}{\pi} \tan^{-1} x \Big|_{-\infty}^{\infty} = \frac{1}{\pi} \left(\tan^{-1} \infty - \tan^{-1}(-\infty)\right)$$

$$= \frac{1}{\pi} \left(\frac{\pi}{2} - \left(\frac{-\pi}{2}\right)\right) = 1$$

In the limit then, the Fourier transform of a constant of magnitude 1 has been shown to have infinite amplitude and unity area at wavenumber $\sigma = 0$ and to be zero elsewhere. This is the definition of the delta function. Thus,

$$F\{1\} = \delta(\sigma)$$

APPENDIX C

DERIVATION OF DISCRETE FOURIER TRANSFORM

Starting with equation (7),

$$\gamma(x)\Delta(x)A(x) = \sum_{k=-\frac{N}{2}}^{\left(\frac{N}{2}\right)-1} \gamma(x)d(x-k\Delta x) = \tilde{\gamma}(x)$$

there is the need to compute its Fourier transform. Because the data is known at discrete points and because of the computer's obvious advantages for doing complex arithmetic manipulations, it is advantageous to compute the transform at discrete points. The discrete Fourier transform equation is derived as follows. If $\tilde{\gamma}(x)$ is the x domain function to be transformed, we can use the expression in Appendix A. The α_n coefficients can be calculated as

$$\alpha_n = \frac{1}{x_o} \int_{-x_o/2}^{x_o/2} \tilde{\gamma}(x) e^{-i2\pi \frac{n}{x_o} x} dx$$

$$= \frac{1}{x_o} \int_{-x_o/2}^{x_o/2} \left[\sum_{k=-\frac{N}{2}}^{\left(\frac{N}{2}\right)-1} \gamma(x)\delta(x-k\Delta x) \right] e^{-i2\pi\left(\frac{n}{x_o}\right)x} dx$$

$$= \frac{1}{x_o} \sum_{k=-\frac{N}{2}}^{\left(\frac{N}{2}\right)-1} \gamma(k\Delta x) \int_{-x_o/2}^{x_o/2} \delta(x-k\Delta x) e^{-i2\pi\left(\frac{n}{x_o}\right)x} dx$$

So

$$\alpha_n = \frac{1}{x_0} \sum_{k=-\frac{N}{2}}^{\left(\frac{N}{2}\right)-1} \gamma(k\Delta x) e^{-i2\pi \frac{n}{x_0}(k\Delta x)}$$

Thus,

$$F\{\tilde{\gamma}(x)\} = \sum_{n=-\infty}^{\infty} \alpha_n \, \delta(\sigma - \frac{n}{x_0})$$

$$= \sum_{n=-\infty}^{\infty} \left[\frac{1}{x_0} \sum_{k=-\frac{N}{2}}^{\left(\frac{N}{2}\right)-1} \gamma(k\Delta x) e^{-i2\pi n \frac{k\Delta x}{x_0}} \right] \delta(\sigma - \frac{n}{x_0})$$

n is the index of variation in the spectral domain and the delta functions are separated by wavenumber intervals of $\frac{1}{x_0}$.

Discrete Fourier transforms, when implemented in digital computers, can be made much more efficient if particular parameter choices are made (Chamberlain, 1979, pp. 315-325). First, if x_c is set equal to X_t, the total path difference traversed by the interferometer, then

$$\frac{\Delta x}{x_0} = \frac{\Delta x}{X_t} = \frac{1}{N}$$

where N is the total number of interferogram samples. Then

$$F\{\tilde{\gamma}(x)\} = \sum_{n=-\infty}^{\infty} \frac{1}{X_t} \sum_{k=-\frac{N}{2}}^{\left(\frac{N}{2}\right)-1} \gamma(k\Delta x) e^{-i2\pi nk/N} \delta(\sigma - \frac{n}{X_t})$$

The α_n coefficients are sampled at intervals of $\frac{1}{X_t}$ wavenumbers. The discrete Fourier transform is additionally simplified if the range that n is allowed to assume is limited to N values. The impact of this decision is analyzed in the following calculation. Let $n = r$.

$$F\{\tilde{\gamma}(x)\}_{n=r} = P(r\Delta\sigma) = \frac{1}{X_t} \sum_{k=-\frac{N}{2}}^{\left(\frac{N}{2}\right)-1} \gamma(k\Delta x) e^{-i2\pi rk/N} \delta(\sigma - \frac{r}{X_t})$$

If $n = r + N$,

$$F\{\tilde{\gamma}(x)\}_{n=r+N} = P((r+N)\Delta\sigma) = \frac{1}{X_t} \sum_{k=-\frac{N}{2}}^{\left(\frac{N}{2}\right)-1} \gamma(k\Delta x) e^{-i2\pi (r+N)\frac{k}{N}} \delta(\sigma - \frac{(r+N)}{X_t})$$

But

$$e^{-i2\pi(r+N)k/N} = e^{-i2\pi rk/N} e^{-i2\pi k} = e^{-i2\pi rk/N} (\cos 2\pi k - i\sin 2\pi k)$$

$$= e^{-i2\pi rk/N} \quad \text{for k an integer}$$

$$F\{\tilde{\gamma}(x)\}_{n=r+N} = \frac{1}{X_t} \sum_{k=-\frac{N}{2}}^{\left(\frac{N}{2}\right)-1} \gamma(k\Delta x) e^{-i2\pi rk/N} \delta(\sigma - \frac{(r+N)}{X_t})$$

That is, at $\sigma = (r+N)\Delta\sigma$, the discrete Fourier transform yields the same result as for $\sigma = r\Delta\sigma$. If N samples are examined, all of the information available from the transform will be recovered.

The discrete transform equation then is given by

$$P(n\Delta\sigma) = \sum_{k=-\frac{N}{2}}^{\left(\frac{N}{2}\right)-1} \gamma(k\Delta x) e^{-i2\pi nk/N} \qquad n = 0,1,2,\ldots,N-1$$

This replication also holds for $n = r-N$ and for positive and negative multiples of N. That is,

$$P(n\Delta\sigma) = P[(n + jN)\Delta\sigma] \quad j = 0, \pm1, \pm2,...$$

In particular, it is important to note that

$$P[(N-n)\Delta\sigma] = P(-n\Delta\sigma)$$

That is, the computed spectrum from wavenumber samples $\frac{N}{2}$ to N is the same spectrum that lies between $\frac{-N\Delta\sigma}{2}$ and 0.

APPENDIX D

SIMULATION PROGRAM

```
C          PROGRAM FTSSIM.FR
C          WRITTEN BY C. L. PARSONS (CODE 971) ON 10/14/82
C
C          DESIGNED TO COMPUTE PERFORMANCE CHARACTERISTICS OF A
C          FLEXIBLE, COMPUTER-CONTROLLED FOURIER TRANSFORM SPECTROMETER
C          GIVEN THE FOLLOWING INPUTS:
C               SIGMAX - UPPER WAVENUMBER CUTOFF OF INCOMING LIGHT
C                        SIGNAL SPECTRUM (IN CM-1)
C               SIGMIN - LOWER WAVENUMBER CUTOFF (IN CM-1)
C               DELSIG - DESIRED SPECTRAL RESOLUTION (IN CM-1)
C               PD     - EXTERNALLY CONTROLLED INTERFEROGRAM
C                        SAMPLING PERIOD (IN MSEC)
C               HR     - HEATING RATE OF OPTICAL TRANSLATION
C                        MECHANISM (IN ZERO-CROSSINGS/MSEC)
C               XBAR   - LASER REFERENCE SIGNAL ZERO-CROSSING PATH
C                        DIFFERENCE = .3164 MICRONS
C               DELN   - NUMBER OF FINAL SAMPLES NEEDED TO CUSHION
C                        THE CENTERING OF INTERFEROGRAM (IN PERCENT
C                        OF N)
C
C          THE OUTPUT PRODUCTS ARE:
C               SIGMAX1 - UPPER WAVENUMBER CUTOFF OF MEASURED
C                         SPECTRUM (IN CM-1)
C               M       - SPECTRAL ORDER
C               DELX    - INTERFEROGRAM SAMPLING INTERVAL (IN MICRONS)
C               YEXTRA  - NO. OF FINAL SAMPLES/ZERO-CROSSING
C               N       - NO. OF FINAL SAMPLES USED IN FFT PROCESS
C               MTOTAL  - NO. OF ORIGINAL SAMPLES NEEDED TO PRODUCE N
C               XTOTAL  - TOTAL TRANSLATION DISTANCE NEEDED (IN MM)
C               TTOTAL  - TOTAL TIME REQUIRED FOR TRANSLATION (IN SEC)
C               R       - NO. OF ORIGINAL SAMPLES/FINAL SAMPLE
C               RPRIME  - NO. OF ORIGINAL SAMPLES/ZERO-CROSSING
C
      REAL MTOTAL
C
C          READ IN INPUTS
C
   10 TYPE ' ENTER THE APPROXIMATE UPPER WAVENUMBER CUTOFF '
      READ FREE (11,ERR=10) SIGMAX
   15 TYPE ' ENTER THE APPROXIMATE LOWER WAVENUMBER CUTOFF '
      READ FREE (11,ERR=15) SIGMIN
   20 TYPE ' ENTER THE DESIRED FINAL OUTPUT SPECTRAL RESOLUTION (CM-1) '
      READ FREE (11,ERR=20) DELSIG
      TYPE ' THE CALCULATIONS ASSUME THAT A HE-NE LASER IS USED '
      TYPE ' THIS IMPLIES A REFERENCE ZERO-CROSSING PATH DIFFERENCE '
      TYPE ' OF .3164 MICRONS '
      WRITE (10,25)
   25 FORMAT (//' IT IS ALSO ASSUMED THAT EXTRA SAMPLES ARE NEEDED ')
      TYPE ' TO ENSURE THAT A CENTERED BLOCK OF DATA CAN BE EXTRACTED '
      TYPE ' FROM THE RAW DATA FILE '
      TYPE ' THE DEFAULT VALUE FOR THE NUMBER OF EXTRA SAMPLES IS '
      TYPE ' 10 PERCENT OF THE FINAL SAMPLES NEEDED AS COMPUTED BELOW '
```

```
   30 TYPE ' IF THIS NOT SATISFACTORY, TYPE 1, OTHERWISE 0 '
      READ FREE (11,ERR=30) INUMB
      IF (INUMB.EQ.0) GO TO 40
   35 TYPE ' THE DESIRED PERCENTAGE OF EXTRA SAMPLES IS '
      READ FREE (11,ERR=35) DELN
      GO TO 45
   40 DELN=10.0
   45 CONTINUE
   48 WRITE (10,50)
   50 FORMAT (//' ENTER THE ORIGINAL SAMPLING PERIOD (IN MSEC) ')
      READ FREE (11,ERR=48) PD
   55 TYPE ' ENTER THE HEATED BAR TRANSLATION RATE (0 XING/MSEC) '
      READ FREE (11,ERR=55) HR
C
C           COMPUTE THE ORDER OF THE FOURIER TRANSFORM SPECTRUM
C
      M=INT(SIGMAX/(SIGMAX-SIGMIN))
      IF (M.LT.1) GO TO 800
C
C           COMPUTE THE INTERFEROGRAM SAMPLING INTERVAL DELX,
C           THE NUMBER OF FINAL SAMPLES/ZERO-CROSSING YEXTRA, AND
C           THE UPPER WAVENUMBER CUTOFF OF THE COMPUTED SPECTRUM
C           SIGMAX1
C
   60 DELX=(M*1E4)/(2.0*SIGMAX)
      XBAR=.3164
      WEXTRA=XBAR/DELX
      IF (WEXTRA.LT.1.0) GO TO 70
      YEXTRA=FLOAT(INT(WEXTRA)+1)
      GO TO 75
   70 YEXTRA=FLOAT(INT(1.0/WEXTRA))
      YEXTRA=1.0/YEXTRA
   75 CONTINUE
      DELX=XBAR/YEXTRA
      SIGMAX1=(M*1E4)/(2.0*DELX)
C
C           CHECK IF SIGMIN IS WITHIN THE RANGE FOR THIS SPECTRAL ORDER
C
      SIGMIN1=SIGMAX1-(1E4/(2.*DELX))
      IF (SIGMIN1.GT.SIGMIN) GO TO 300
C
C           COMPUTE THE NUMBER OF FINAL SAMPLES N NEEDED FOR FFT
C
      XN=1E4/(DELSIG*DELX)
      K=INT(ALOG(XN)/ALOG(2.))+1
      N=IFIX(EXP(K*ALOG(2.)))
C
C           COMPUTE THE TOTAL NUMBER OF ORIGINAL SAMPLES NEEDED
C           TO GET N FINAL SAMPLES
C
      MTOTAL=((1.0+(DELN/100.0))*N)/(PD*HR*YEXTRA)
C
C           COMPUTE THE TOTAL PATH DIFFERENCE, THE TOTAL SCAN TIME,
C           THE NUMBER OF ORIGINAL SAMPLES/FINAL SAMPLE, AND THE
C           NUMBER OF ORIGINAL SAMPLES/ZERO-CROSSING
C
```

```
      XTOTAL=MTOTAL*DELX*1E-3
      TTOTAL=MTOTAL*PD*1E-3
      R=MTOTAL/((1.0+(DELN/100.0))*N)
      RPRIME=R*YEXTRA
C
C          PRINT OUT RESULTS TO LIST FILE
C
  100 FORMAT (1H1)
  105 FORMAT ( ' FOR A DESIRED WAVENUMBER WINDOW FROM ',F10.2,
     *' CM-1 TO ',E10.2,' CM-1 ' )
  108 FORMAT ( '       (OR ',F8.2,'A TO ',F8.2,'A). ' )
  110 FORMAT ( ' AND A SPECTRAL RESOLUTION OF ',F7.2,' CM-1 ' )
  112 FORMAT ( '       (OR ',F7.3,'A AT 5000A) ' )
  115 FORMAT ( ' THE FOLLOWING FOURIER TRANSFORM SPECTROMETER DESIGNS ' )
  120 FORMAT ( ' ARE POSSIBLE: '///)
  125 FORMAT ( ' (THE LASER REFERENCE CHANNEL ZERO-CROSSING PATH ' )
  130 FORMAT ( ' DIFFERENCE IS ASSUMED TO BE .3164 MICRONS ) '//)
  135 FORMAT ( ' HARDWARE VARIABLES -- '/)
  140 FORMAT ( ' THE PULSE GENERATOR SAMPLING PERIOD = ',F5.1,' MSEC ')
  145 FORMAT ( ' THE BAR HEATING RATE = ',F6.3,' ZERO-CROSSING/MSEC '/)
  150 FORMAT ( ' SOFTWARE VARIABLES -- '/)
  155 FORMAT ( ' FOR SPECTRAL ORDER ',I1)
  160 FORMAT ( '     THE OUTPUT SPECTRUM UPPER CUTOFF = ',F10.2,
     *' CM-1 ')
  162 FORMAT ( '     THE OUTPUT SPECTRUM LOWER CUTOFF = ',F10.2,' CM-1 ' )
  165 FORMAT ( '     THE PATH DIFFERENCE INTERVAL = ',E7.4,' MICRONS ')
  170 FORMAT ( '     THIS REQUIRES A SAMPLING RATE/ZERO-CROSSING = ',
     *F6.3)
  175 FORMAT ( '     THE NUMBER OF POINTS NEEDED FOR THE FFT = ',I5/)
  180 FORMAT ( '     ASSUMING A CUSHION EQUAL TO ',F5.1,
     *' PERCENT OF THIS NUMBER OF POINTS, ' )
  185 FORMAT ( '     A TOTAL OF ',E8.2,' ORIGINAL SAMPLES IS NEEDED '/)
  190 FORMAT ( '     THE TOTAL TRANSLATION PATH DIFFERENCE = ',F7.4,
     *' MM ')
  195 FORMAT ( '     AND THE TOTAL TIME NEEDED/SCAN = ',F8.4,' SEC')
  200 FORMAT ( '     THE NUMBER OF ORIGINAL SAMPLES/FINAL SAMPLE = ',
     *F8.4)
  205 FORMAT ( '     AND THE NUMBER OF ORIGINAL SAMPLES/ZERO-CROSSING =',
     *F8.4)
      WRITE (12,100)
      WRITE (12,105) SIGMIN,SIGMAX
      WLMIN=(1.0/SIGMIN)*1E8
      WLMAX=(1.0/SIGMAX)*1E8
      WRITE (12,108) WLMIN,WLMAX
      WRITE (12,110) DELSIG
      DELWL=DELSIG*.25
      WRITE (12,112) DELWL
      WRITE (12,115)
      WRITE (12,120)
      WRITE (12,125)
      WRITE (12,130)
      WRITE (12,135)
      WRITE (12,140) PD
      WRITE (12,145) HR
      WRITE (12,150)
      WRITE (12,155) M
```

```
      WRITE (12,160) SIGMAX1
      WRITE (12,162) SIGMIN1
      WRITE (12,165) DELX
      WRITE (12,170) YEXTRA
      WRITE (12,175) N
      WRITE (12,180) DELN
      WRITE (12,185) MTOTAL
      WRITE (12,190) XITOTAL
      WRITE (12,195) TTOTAL
      WRITE (12,200) R
      WRITE (12,205) RPRIME
C
C           FOR M.GT.1 LOOP BACK FOR OTHER ORDERS
C
      IF (M.GT.1) GO TO 300
      GO TO 400
  300 M=M-1
      GO TO 60
C
C           DECIDE IF OTHER CASES ARE TO BE RUN
C
  400 TYPE ' IF OTHER CASES ARE TO BE RUN, TYPE 1,OTHERWISE 0 '
      READ FREE (11,ERR=400) INUMB
      IF (INUMB.EQ.0) GO TO 960
      GO TO 10
C
C           WRAPUP
C
  800 TYPE ' A SPECTRAL ORDER LESS THAN 1 WAS COMPUTED - ABORT '
  960 CONTINUE
      STOP
      END
```